

Supplemental Information

Formation and Maintenance of Mesenchymal and Stem-Cell States in the Breast by Paracrine and Autocrine Signals

Christina Scheel, Elinor Ng Eaton, Sophia Hsin-Jung Li, Christine L. Chaffer, Ferenc Reinhardt, Kong-Jie Kah, George Bell, Wenjun Guo, Jeffrey Rubin, Andrea L. Richardson and Robert A. Weinberg

Figure S1. A mesenchymal subpopulation (MSP) isolated from immortalized human mammary epithelial (HMLE) cells.

(A) Bright phase images: MSP cells were detected floating as small, epithelial sheets on top of adherent HMLE monolayer cultures. When isolated from HMLE cultures, these cells re-attached and were subsequently propagated as adherent monolayer cultures with a mesenchymal morphology. (B) RT-PCR: mRNA expression of EMT-TFs, E- and N-cadherin in HTwist and MSP, all relative to HMLE²⁴⁺ cells. (C) Secreted protein profiling: experimental design: cell culture supernatant collected from HMLE²⁴⁺ and HTwist cells was filtered and biotinylated. Three dilutions (2x-10x-20x) of culture supernatant were incubated with antibody arrays. (D) Heat-map of 10% top differentially secreted proteins in HTwist compared to HMLE²⁴⁺ cells, based on consistent performance of each listed antibody for the three dilutions of cell culture supernatant (2x-10x-20x). (E) ELISA: to serve as a quality control for the antibody array, for selected proteins we compared the difference in signal intensity between HMLE²⁴⁺ and HTwist cells on the antibody array and fold-difference in absolute protein levels measured by ELISA.

Figure S2. EMT-associated autocrine signaling.

(A) RT-PCR: mRNA expression of BMP ligands in HMLE²⁴⁺, HTwist and MSP cells, n=3. (B) Luciferase reporter assay: Smad transcriptional activity: cells were transfected with SBE4-luc reporter plasmid, firefly luciferase levels were normalized to pGL-SV40 renilla transfection control; cells were treated with recombinant TGF- β 1 (5ng/ml) for 30min, n=3. (C) RT-PCR: mRNA expression of SFRP isoforms in HMLE²⁴⁺ and MSP cell lines, n=3. (D) RT-PCR: mRNA expression of Wnt ligands in HMLE²⁴⁺, HTwist and MSP cell lines, n=3. (E) Summary of

differential expression of secreted proteins regulating Wnt, TGF- β and BMP pathways in HMLE²⁴⁺, HTwist and MSP cell lines.

Figure S3. Autocrine Signaling controls migration and mammosphere formation

(A) Growth curves: proliferation assay (MTS) of MSP and HTwist cell lines treated every 24h for a duration of 4d with recombinant DKK1 (1 μ g/ml), SFRP1 (1 μ g/ml) or BMP4 protein (0.5 μ g/ml), n=4. (B) Immunoblot: inhibition of constitutive Smad2 phosphorylation in MSP cells by TGFBR1-kinase inhibitors A83-01 and SB43(1542), added at a concentration of 10 μ M for 30min. Loading control: total Smad2/3. (C) Immunofluorescence: inhibition of nuclear translocation of Smad2/3 by A83-01 or SB43 (10 μ M) in HMLE²⁴⁺ cells treated concomitantly with 2.5ng/ml TGF- β 1, cells were fixed 30min after addition of factors. (D) Mammosphere Assay: HTwist and MSP were treated daily during mammosphere formation (5d) with BMP4 (0.5 μ g/ml), SB43 (10 μ M) or a combination of both (B+S), n=6 wells. (E) Migration Assay: HTwist and MSP cells were seeded into Boyden Chambers in the presence of A83-01 and SB43 (10 μ M), n=3 wells. (F) Bright field microscopy images of HMLE-Twist-ER untreated control cells (-HTX), and treated with 20nM hydroxytamoxifen daily for 12d (+HTX). (G) Mammosphere assay: HMLE-Twist-ER cells treated with HTX for 12d and untreated control cells were plated in mammosphere assays in the absence of further HTX treatment. SFRP1 (1 μ g/ml) or BMP4 protein (0.5 μ g/ml) were added every 24h singly or in combination (S+B) during mammosphere formation (5d), n=8 wells. (H) Migration assay: HTX-treated and control HMLE-Twist-ER cells were plated in Boyden Chambers and treated analogous to (G), n=3 wells.

Figure S4. Autocrine Signaling controls tumorigenicity and metastasis

(A) Flow cytometry: CD44-APC and CD24-PE cell surface marker expression in RAS-transformed HMLE²⁴⁺, HTwist and MSP cells. Numbers indicate % of the CD44^{hi}/CD24⁻ population. (B) Tumorigenicity assay: HMLE²⁴⁺-RAS, HTwist-RAS, MSP-RAS, or HMLE²⁴⁺ and MSP cells were implanted subcutaneously at indicated numbers in mice. Mice were euthanized and necropsied after 10 weeks. (C) Lung metastasis: fluorescent images of GFP-positive metastatic foci: HMLE²⁴⁺-RAS, MSP-RAS and independently isolated and transformed MSP-II-RAS cells were implanted in the fat pads of mice. (D) Quantification of lung surface metastatic foci, shown are metastases/lung lobe, n=5 mice/group. (E) Lung colonization assay: fluorescent images of GFP-positive metastatic foci: HMLE²⁴⁺-RAS and MSP-RAS cells were injected via tail vein. (F) Histology of macroscopic lung metastases, hematoxylin and eosin staining. Tumor cells have much larger nuclei compared to murine lung epithelium: HMLE²⁴⁺-RAS cells form ductal structures, MSP-RAS cells grow diffusively with no distinct border to lung epithelium. (G) Quantification of lung surface metastatic foci, shown are metastases/lung lobe, n=10 mice/group. (H) Proliferation Assay. MSP-RAS cells were treated daily for 5d with SFRP1 (1µg/ml), BMP4 (0.5µg/ml), protein or a combination of both, cumulative proliferation over 5d was measured by the MTS assay, n=6. (I) Flow cytometry: CD44-APC and CD24-PE cell-surface markers of dissociated primary tumorspheres (after treatment as described in Figure 4B). Numbers indicate % of CD44^{hi}/CD24⁻ (upper right quadrant) and CD44^{-med}/CD24⁺ (lower right quadrant) (J) Histology of primary tumors from dissociated primary tumorspheres (after treatment as described in Figure 4B): no major differences in tumor histology were observed between different groups.

Figure S5. Creation of a permissive extracellular environment for EMT-induction

(A) Immunoblot: Smad2 phosphorylation in HMLE²⁴⁺ cells. Protein was extracted 30min after treatment with indicated concentrations of recombinant TGF- β 1; loading control: β -actin. (B) RT-PCR: mRNA expression of SFRP1 in HMLE²⁴⁺ cells stably expressing two hairpin-encoding vectors (shSFRP1a and shSFRP1b) compared to cells expressing a control hairpin targeting GFP (shGFP), HMLE²⁴⁺shSFRP1b cells were used for EMT-induction experiments. (C) RT-PCR: mRNA levels of ZEB2 relative to untreated control: concomitant knockdown of SFRP1 (shSFRP1) and addition of anti-DKK1 (10 μ g/ml) antibody allow TGF- β 1 (2.5ng/ml) to induce expression of EMT-TF ZEB2 in HMLE²⁴⁺ cells. (D) RT-PCR: mRNA levels of ZEB2 relative to untreated control: concomitant knockdown of SFRP1 (shSFRP1) and addition of anti-DKK1 (10 μ g/ml) antibody allow BMP-antagonist Gremlin (2.5ug/ml) or Wnt5a (250ng/ml) to promote TGF- β -induced expression of EMT-TF ZEB2. (E) Bright phase microscopy: images of untreated control cells (HMLE²⁴⁺-shGFP and -shSFRP1), HMLE²⁴⁺-shGFP cells treated with TGF- β 1 (2.5ng/ml), HMLE²⁴⁺-shSFRP1 cells treated with the EMT induction cocktail (IC): TGF- β 1 (2.5ng/ml), Wnt5a (250ng/ml), anti-DKK1- (10 μ g/ml) and anti-E-cadherin-antibody (1 μ g/ml). Factors were added every 48h. (F) Growth curves: proliferation of phenotypically stable, indicated cell lines was monitored by the MTS assay for 3d, 8 passages after cessation of a 14d treatment as described in (E), n=12. (G) RT-PCR: mRNA expression of ZEB1, ZEB2, E-cadherin and N-cadherin, all relative to HMLE²⁴⁺-shGFP control cells. Shown are PBS-treated control HMLE²⁴⁺-shGFP and HMLE²⁴⁺-shSFRP1 cells, 2 replicates of HMLE²⁴⁺-shGFP cultures treated with TGF- β 1 (a and b), and 2 replicates of HMLE²⁴⁺-shSFRP1 cultures treated with the IC (a and b). mRNA was isolated 8 passages after cessation of a 14d treatment as described in (E). (H) Luciferase reporter assay: indicated cells were transfected with smad (SBE4) and β -

catenin/TCF-LEF (TOPFLASH) reporter plasmids, reporter assays were conducted 8 passages after cessation of 14d treatment as described in (E), n=3. (I) Immunoblot: EMT markers and associated autocrine pathways, protein was extracted 8 passages after cessation of 14d treatment as described in (E).

Figure S6. Characterization of primary mammary epithelial cell populations that are enriched in self-renewal and motility

(A) FACS: single-cell preparations were obtained from human reduction mammoplasties; (1.) dead cells were excluded by 7AAD staining, followed by (2.) exclusion of cells positive for CD45 (white blood cells) and CD31 (endothelial cells). (3.) Using the resultant Lin⁻ cells, MEC^{EPC⁻} (CD49⁺/EpCAM⁻) and MEC^{EPC⁺} (CD49⁺/EpCAM⁺) populations were collected. (B) Bright phase microscopy: FACS-purified MEC^{EPC⁻}, MEC^{EPC⁺} and unsorted MEC were cultured for 5d. (C) RT-PCR: mRNA expression of Claudin-2 (CLDN2), ZO-1 and E-cadherin (E-cad) in cultured MEC^{EPC⁻} and MEC^{EPC⁺} 5d after FACS. (D) RT-PCR: mRNA expression of p63 and EMT TFs in in cultured MEC^{EPC⁻} and MEC^{EPC⁺} 5d after FACS. (E) Mammosphere assay: MEC^{EPC⁻} migrated cells were collected from the bottom of Boyden Chambers by trypsinization and their mammosphere forming ability compared to parental MEC^{EPC⁻} and MEC^{EPC⁺}, n=24 wells. (F) Immunofluorescence: purified MEC^{EPC⁻}, MEC^{EPC⁺} cultured for 5d after FACS: differential expression of myoepithelial lineage marker alpha-smooth muscle actin (alpha-SMA, expressed in <1/100 cells/well), basal lineage markers cytokeratin 14 (CK14) and p63. Differential expression of luminal lineage markers mucin 1 (MUC1), cytokeratin 8 (CK8), CK18. (H) RT-PCR: Axin2 mRNA expression in cultured MEC^{EPC⁻} and MEC^{EPC⁺}, 5d after FACS. (G) Immunofluorescence: membranous and cytoplasmic/nuclear localization of β -catenin

in cultured MEC^{EPC-} and MEC^{EPC+}, 5d after FACS (I) Growth curve: MEC^{EPC-} treated every 24h with indicated factors: TGF- β receptor I (TGFBR1)-kinase inhibitors A83-01 and SB43(1542) (10 μ M), SFRP1 (1 μ g/ml); cells were counted at indicated time points, n=2.

Figure S7. Wnt and TGF- β signals govern interconversions between SC-enriched, basal and lineage-restricted, luminal MEC

(A) Mammosphere assay: MEC^{EPC-} were seeded into the mammosphere assay after a 5d pretreatment with TGF- β receptor I (TGFBR1)-kinase inhibitors A83-01 (3 μ M) and recombinant SFRP1 (300ng/ml) or a combination of both (A+S) in monolayer culture, inhibitors were added every 24h, n=12 wells. (B) RT-PCR: mRNA expression of Slug, Claudin-2 (CLDN2) and p63 in MEC^{EPC-} following treatment as described in (A), and MEC^{EPC+}, all relative to untreated control MEC^{EPC-}. (C) Immunofluorescence: expression of E-cadherin, ZO-1, Slug and p63 in MEC^{EPC-} 2d after a 5d treatment as described in (A). (D) Mammosphere assay: MEC^{EPC+} were seeded into the mammosphere assay after a 5d pretreatment in monolayer culture with the following factors, added singly or in indicated combination: recombinant TGF- β 1 (TGF- β , 0.1ng/ml), anti-E-cadherin antibody (α EC, 20 μ g/ml), a mix of Wnt-pathway stimulating factors referred to as WNT (anti-DKK1 antibody (10 μ g/ml), anti-SFRP1 antibody (1 μ g/ml), recombinant Wnt5a (250ng/ml), n=10 wells. (E) Migration Assay: FACS purified MEC^{EPCAM+} were pretreated for 5d as described in (D), shown are migrated cells/field, 5 fields were counted, n=3 wells. (F) Growth curve of MEC^{EPC+} during treatment with factors described in (D), n=2. (G) Growth curve of MEC^{EPC+} during treatment with factors as described in Figure 7A, n=2.

Table S2

Functional group	Antibodies on array		Antibodies Top 50		Enrichment fraction
	n	%	n	%	
Angiogenesis	31	6.1	7	14.0	2.3
Wnt	22	4.3	4	8.0	1.8
FGF	22	4.3	3	6.0	1.4
TGF+BMP	43	8.5	5	10.0	1.2
Chemokines/Cytokines	143	28.2	14	28.0	1.0
Other	216	42.6	16	32.0	0.8
MMP	20	3.9	1	2.0	0.5
IGF	10	2.0	0	0.0	0.0
<i>TOTAL</i>	<i>507</i>	<i>100.0</i>	<i>50</i>	<i>100.0</i>	<i>1.0</i>

Functional grouping of top 50 differentially secreted protein in HTwist cells, for details, see Table S1.

Supplemental Experimental Procedures

Cell Lines

Human mammary epithelial cell lines (HMLE) were generated as described and immortalized using retroviral vectors to express the catalytic subunit of the human telomerase enzyme, hTERT and the SV-40 Large T antigen (Elenbaas et al., 2001). HMLE cells were propagated in MEGM medium (Lonza) according to standard protocols.

In order to compare the autocrine signaling environment of epithelial HMLE to mesenchymal MSP and HTwist cells, we wished to avoid confounding effects caused by the presence of CD44^{hi}/CD24⁻ mesenchymal/SC within bulk HMLE populations. Accordingly, we purified CD24⁺, epithelial cells by MACS, using the Collection Kit for mouse IgG (Invitrogen) for positive selection with a CD24 antibody (BD Biosciences) according to the manufacturers instructions.

Mesenchymal sub-population (MSP) cells were detected as a minority population of free-floating cells in confluent monolayer cultures of HMLE cells. When removed from HMLE cultures, these MSP populations re-adhered in new culture dishes and were subsequently propagated in monolayer cultures.

HMLE-Twist-ER cells were generated as described (Casas et al., 2011). For EMT-induction, 20nM of hydroxytamoxifen (Sigma) in Ethanol was added to the culture medium every 24h for a total duration of 12 days. Untreated control cells received vehicle (Ethanol).

Primary Mammary Epithelial Cell cultures

Single-cell suspensions of primary human mammary epithelial cells (MECs) were generated by collagenase/hyaluronidase digestion from reduction mammoplasties of pre-menopausal women

as previously described with minor modifications (Stingl et al., 2001). Data from 4 donors are included in this study. Primary MEC were cultured on collagen I-coated plates (Millipore) in MEGM medium (Lonza) supplemented with 1% Fetal Bovine Serum or in WIT-P medium (Stemgent) in a humidified 4% O₂, 5% CO₂, atmosphere.

Plasmids, Virus production and infection of target cells

HMLE cells were cells were infected with pBABE-Twist vector to generate HTwist cells as previously described (Yang et al., 2004). To generate tumorigenic and green fluorescent protein (GFP)-expressing HMLE, HTwist and MSP cells, cells were infected with pBabe-V12H-RAS (Elenbaas et al., 2001) and pRRL-GFP vectors. For stable knockdown of SFRP1, pLKO1 small hairpin-expressing vectors were purchased from Open Biosystems (shSRP1_a, clone ID TRCN0000062168, shSFRP1_b, clone ID TRCN00000621672). Production and infection of target cells were previously described (Stewart et al., 2003). Infected cells were selected with 2 µg/mL puromycin, 200 µg/mL hygromycin, and 200 µg/mL neomycin.

Antibody arrays

Culture medium of HMLE²⁴⁺ and HTwist cells was collected following an incubation period of 48h and filtered through a 20µm mesh (BD Falcon). Each sample was biotinylated and hybridized in three dilutions to L-series 500-antibody arrays (Raybiotech). For each array, protein intensity values were background subtracted, scaled by the internal control, and floored at 1 unit. For each dilution, t-test p-values for triplicate arrays were used to rank proteins, and antibodies showing changes in different directions were excluded. The top 10% assayed proteins were selected by mean rank across three dilutions.

ELISA

Culture medium was collected following an incubation period of 48h and filtered through a 20µm mesh (BD Falcon). All ELISAs were performed using commercially available kits according to the manufacturer's instructions. For DKK1, Pentraxin 3, TGF-β1, VEGF-c and uPA, ELISA kits and ancillary products were purchased from R&D systems. All ELISA readouts were normalized by cell number.

Microarray hybridization, data collection, and analysis

Total RNA was extracted from three independent culture plates for HMLE²⁴⁺ and three independently generated MSP cell lines with the RNeasy Mini kit (Qiagen). Synthesis of cRNA and hybridization/scanning of microarrays were done with Affymetrix GeneChip products as described in the GeneChip manual. Raw data (CEL) files were normalized and summarized into probeset values with RMA using Bioconductor (Irizarry et al., 2003). Hierarchical Clustering analysis was performed using the GenePattern software package (Reich et al., 2006) and Hierarchical Clustering module (Eisen et al., 1998) with Pearson correlation performed on both column and rows. The gene expression data for HMLE²⁴⁺ and MSP cells was combined with data for Twist-overexpressing HMLE cells and their corresponding vector-only controls (from GEO accession no. GSE24202, (Taube et al., 2010)). Only a subset of probesets corresponding to an EMT core signature was used for the clustering analysis (Table S3). The resulting heatmap and dendrogram (Table S4) was generated with the Hierarchical Clustering Image module. A moderated t-test was performed for each gene using an empirical Bayes approach (Smyth, 2004), and a p-value was calculated to control for false discovery rate resulting from multiple

hypothesis testing. Only probesets with a $p < 0.01$ for all five cell lines and identical direction of change (up-regulated or down-regulated compared with control cells) were included in the core signature. Microarray data have been deposited in the GEO archive.

Luciferase assays

Reporter Plasmids were previously described: Super 8x TOPFlash, corresponding FOPFlash control plasmid (Veeman et al., 2003) and SBE4-luc (Zawel et al., 1998). 5.0×10^4 cells were co-transfected with 500ng of the indicated firefly luciferase reporter plasmid and 50 ng of pGL-SV40-*Renilla* luciferase normalization control plasmid using Fugene 6 transfection reagent (Roche). Lysates were collected 24-48 hr after transfection, and firefly and *Renilla* luciferase activities were measured with a Dual-Luciferase Reporter System (Promega).

Recombinant proteins and inhibitors

Recombinant human DKK1, SFRP1 and mouse Wnt5a were purchased from R&D Systems. Recombinant BMP4 was obtained from Stemgent. Small molecule inhibitors were from Tocris (A83-01; (Tojo et al., 2005) and Sigma (SB431542; (Laping et al., 2002). Anti-DKK1 antibody was obtained from R&D Systems, anti-E-cadherin antibody (HECD-1) from Invitrogen.

Antibodies

Immunoblotting: Beta-actin, Snail, Twist (Abcam); E-cadherin, N-cadherin (BD Transduction); ZEB1 (Bethyl Labs); phospho-SAPK/JNK (T183/Y185, clone G9), JNK, phospho-c-JUN (S63), JUN, phospho-PKC (pan, beta II/Ser660), Slug (C19G7), phospho-smad2, smad2/3 (Cell Signaling), Wnt5a (R&D Systems).

Immunofluorescence: E-cadherin, smad2/3, Twist, ZEB1, see *Immunoblotting*; alpha-smooth muscle actin-Cy3 (Sigma), beta-catenin, total (BD Transduction), cytokeratin 8 (TROMA-1, Developmental Studies Hybridoma Bank), cytokeratin 14 (AF64, Covance), cytokeratin 18 (DC10, NeoMarkers), MUC-1 (HMPV, BD Pharmingen), pan-cytokeratin (Biogenex), p63 (4A4, Santa Cruz), Vimentin (V9, Sigma), ZO-1 (Invitrogen).

FACS: EpCAM-FITC (StemCell Technologies), CD24-FITC and CD24-PE (BD Pharmingen), CD31-APC (WM59, BD Pharmingen), CD44-APC (BD-Pharmingen) CD45-V450 (BD Horizon), CD49f-PE (BD Pharmingen).

Neutralization of bio-activity: E-cadherin (Invitrogen, Clone HECD-1), DKK1 (R&D Systems), SFRP1, a gift from Jeffrey Rubin (Hausler et al., 2004).

Primers used for RT-PCR

Table S5

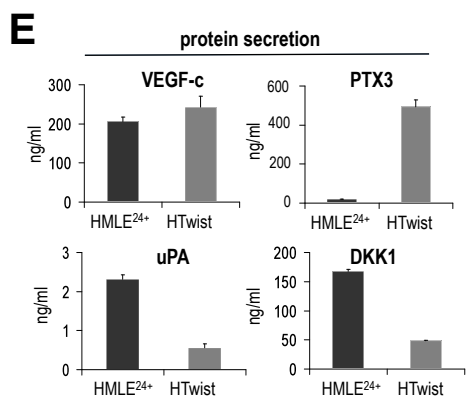
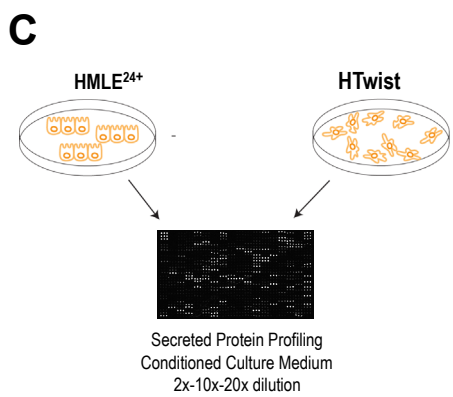
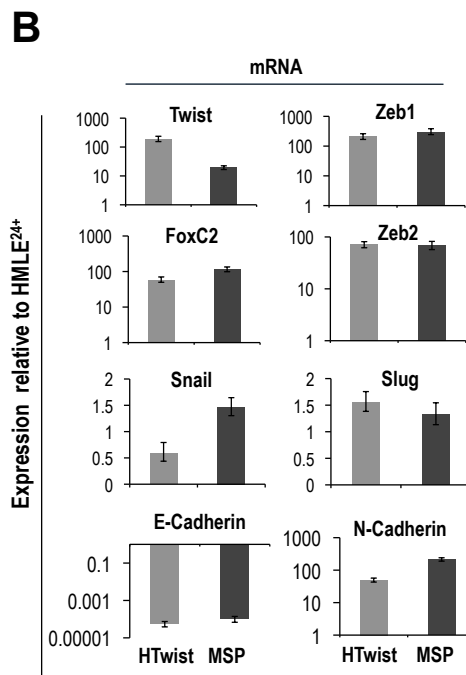
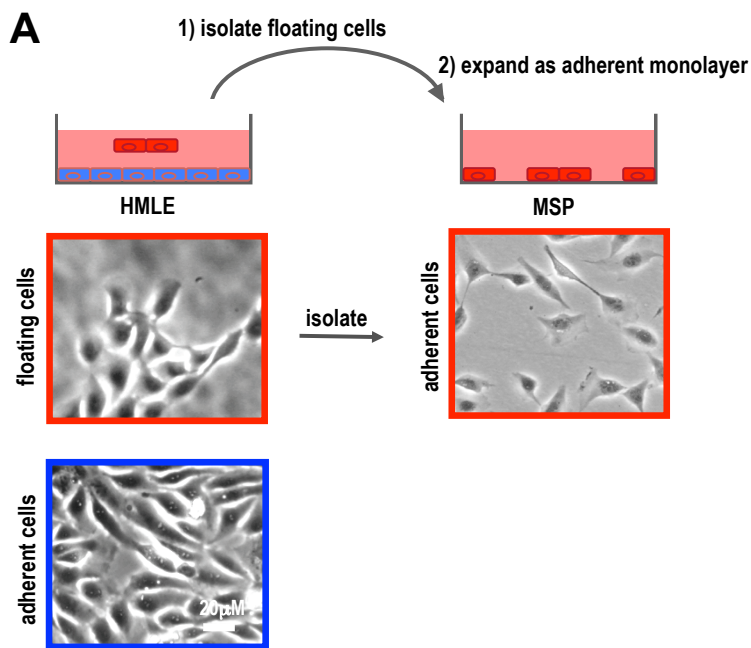
Proliferation Assays

To measure cell growth rates, 1000 cells were seeded onto 96-well plates in triplicate. Cell viability was measured using CellTiter-Glo (Promega) according to the manufacturer's instructions.

Supplementary References

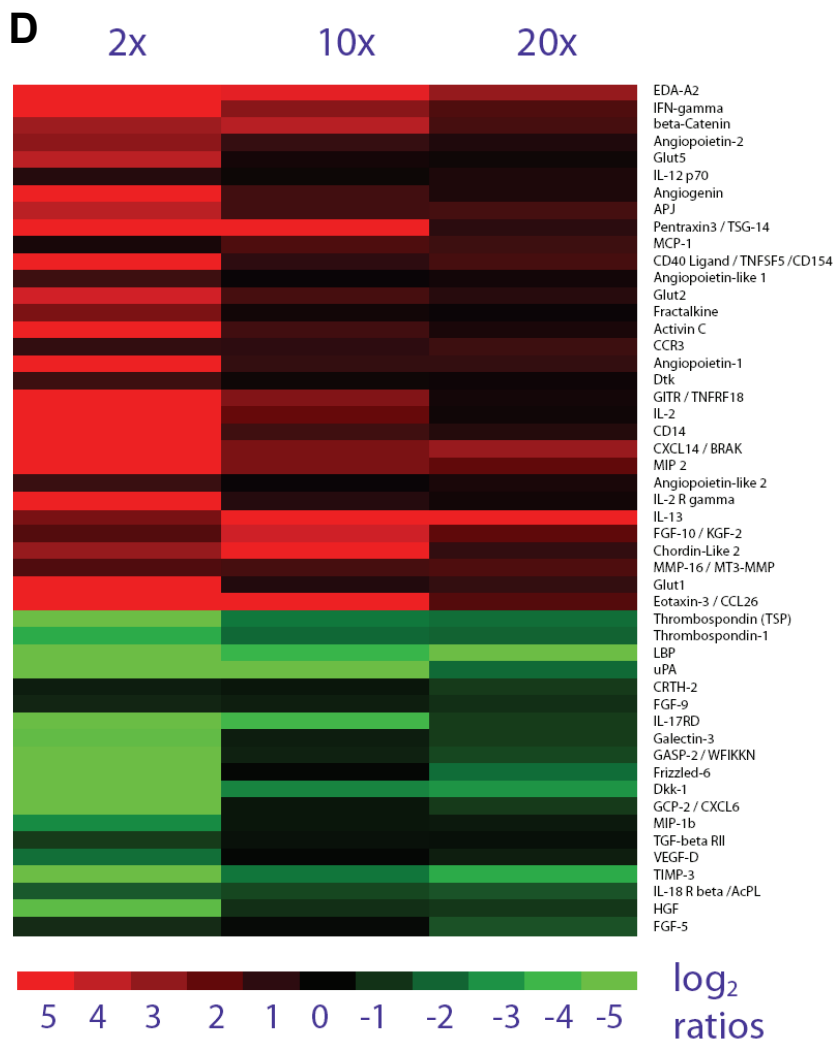
- Casas, E., Kim, J., Bendesky, A., Ohno-Machado, L., Wolfe, C.J., and Yang, J. (2011). Snail2 is an essential mediator of Twist1-induced epithelial mesenchymal transition and metastasis. *Cancer Res* 71, 245-254.
- Eisen, M.B., Spellman, P.T., Brown, P.O., and Botstein, D. (1998). Cluster analysis and display of genome-wide expression patterns. *Proc Natl Acad Sci U S A* 95, 14863-14868.
- Elenbaas, B., Spirio, L., Koerner, F., Fleming, M.D., Zimonjic, D.B., Donaher, J.L., Popescu, N.C., Hahn, W.C., and Weinberg, R.A. (2001). Human breast cancer cells generated by oncogenic transformation of primary mammary epithelial cells. *Genes Dev* 15, 50-65.
- Hausler, K.D., Horwood, N.J., Chuman, Y., Fisher, J.L., Ellis, J., Martin, T.J., Rubin, J.S., and Gillespie, M.T. (2004). Secreted frizzled-related protein-1 inhibits RANKL-dependent osteoclast formation. *J Bone Miner Res* 19, 1873-1881.
- Irizarry, R.A., Hobbs, B., Collin, F., Beazer-Barclay, Y.D., Antonellis, K.J., Scherf, U., and Speed, T.P. (2003). Exploration, normalization, and summaries of high density oligonucleotide array probe level data. *Biostatistics* 4, 249-264.
- Laping, N.J., Grygielko, E., Mathur, A., Butter, S., Bomberger, J., Tweed, C., Martin, W., Fornwald, J., Lehr, R., Harling, J., *et al.* (2002). Inhibition of transforming growth factor (TGF)-beta1-induced extracellular matrix with a novel inhibitor of the TGF-beta type I receptor kinase activity: SB-431542. *Mol Pharmacol* 62, 58-64.
- Reich, M., Liefeld, T., Gould, J., Lerner, J., Tamayo, P., and Mesirov, J.P. (2006). GenePattern 2.0. *Nat Genet* 38, 500-501.
- Smyth, G.K. (2004). Linear models and empirical bayes methods for assessing differential expression in microarray experiments. *Statistical applications in genetics and molecular biology* 3, Article3.
- Stewart, S.A., Dykxhoorn, D.M., Palliser, D., Mizuno, H., Yu, E.Y., An, D.S., Sabatini, D.M., Chen, I.S., Hahn, W.C., Sharp, P.A., *et al.* (2003). Lentivirus-delivered stable gene silencing by RNAi in primary cells. *Rna* 9, 493-501.
- Stingl, J., Eaves, C.J., Zandieh, I., and Emerman, J.T. (2001). Characterization of bipotent mammary epithelial progenitor cells in normal adult human breast tissue. *Breast Cancer Res Treat* 67, 93-109.
- Taube, J.H., Herschkowitz, J.I., Komurov, K., Zhou, A.Y., Gupta, S., Yang, J., Hartwell, K., Onder, T.T., Gupta, P.B., Evans, K.W., *et al.* (2010). Core epithelial-to-mesenchymal transition interactome gene-expression signature is associated with claudin-low and metaplastic breast cancer subtypes. *Proc Natl Acad Sci U S A* 107, 15449-15454.
- Tojo, M., Hamashima, Y., Hanyu, A., Kajimoto, T., Saitoh, M., Miyazono, K., Node, M., and Imamura, T. (2005). The ALK-5 inhibitor A-83-01 inhibits Smad signaling and epithelial-to-mesenchymal transition by transforming growth factor-beta. *Cancer Sci* 96, 791-800.
- Veeman, M.T., Slusarski, D.C., Kaykas, A., Louie, S.H., and Moon, R.T. (2003). Zebrafish prickles, a modulator of noncanonical Wnt/Fz signaling, regulates gastrulation movements. *Curr Biol* 13, 680-685.
- Yang, J., Mani, S.A., Donaher, J.L., Ramaswamy, S., Itzykson, R.A., Come, C., Savagner, P., Gitelman, I., Richardson, A., and Weinberg, R.A. (2004). Twist, a master regulator of morphogenesis, plays an essential role in tumor metastasis. *Cell* 117, 927-939.

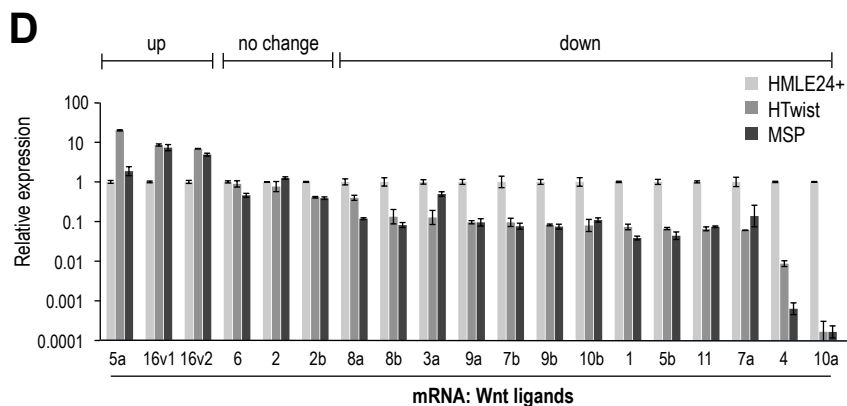
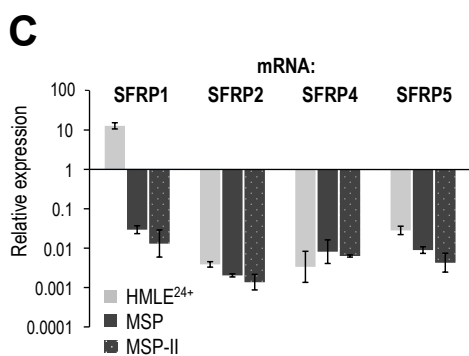
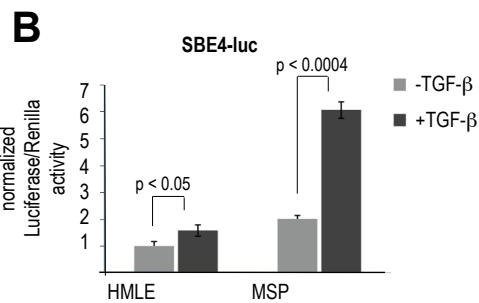
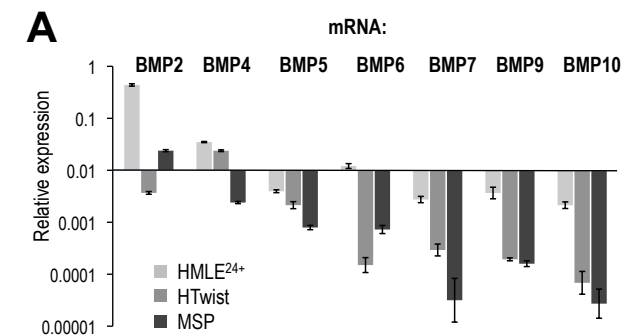
Zawel, L., Dai, J.L., Buckhaults, P., Zhou, S., Kinzler, K.W., Vogelstein, B., and Kern, S.E. (1998). Human Smad3 and Smad4 are sequence-specific transcription activators. *Mol Cell* 1, 611-617.



	Array	ELISA
VEGF-c	1.2	1.2
PTX3	2.8	25.6
uPA	2.5	4.5
DKK1	0.7	0.3

fold change HMLE/HTwist





E

Protein	Function	Down in MSP	Down in HTwist	Up in HTwist	Up in MSP	Method of Detection
DKK1*	Wnt antagonist	x	xx			ELISA
SFRP1**	Wnt antagonist	xx	x			RT-PCR
Chordin-like2*	BMP antagonist			x	x	RT-PCR
Gremlin1**	BMP antagonist			x	xx	RT-PCR
Wnt5a**	Wnt ligand, non-canonical			xx	x	Western Blot
Wnt16	Wnt ligand, non-canonical			x	x	RT-PCR
Wnt1	Wnt ligand, canonical	xx	x			RT-PCR
Wnt4	Wnt ligand, canonical	xx	x			RT-PCR
Wnt5b	Wnt ligand, non-canonical	x	x			RT-PCR
Wnt7a	Wnt ligand, canonical	x	xx			RT-PCR
Wnt8a	Wnt ligand, canonical	xx	x			RT-PCR
Wnt8b	Wnt ligand, canonical	x	x			RT-PCR
Wnt10	Wnt ligand, non-canonical	x	x			RT-PCR
BMP2	Bmp ligand	x	x			RT-PCR
BMP4	Bmp ligand	xx	x			RT-PCR
BMP5	Bmp ligand	x	xx			RT-PCR
BMP6	Bmp ligand	x	x			RT-PCR
BMP7	Bmp ligand	xx	x			RT-PCR
BMP9	Bmp ligand	xx	x			RT-PCR
BMP10	Bmp ligand	x	xx			RT-PCR
TGF-beta1	TGF-beta ligand			x	xx	ELISA

* first revealed by protein array, **first revealed by gene expression profiling

Figure S3

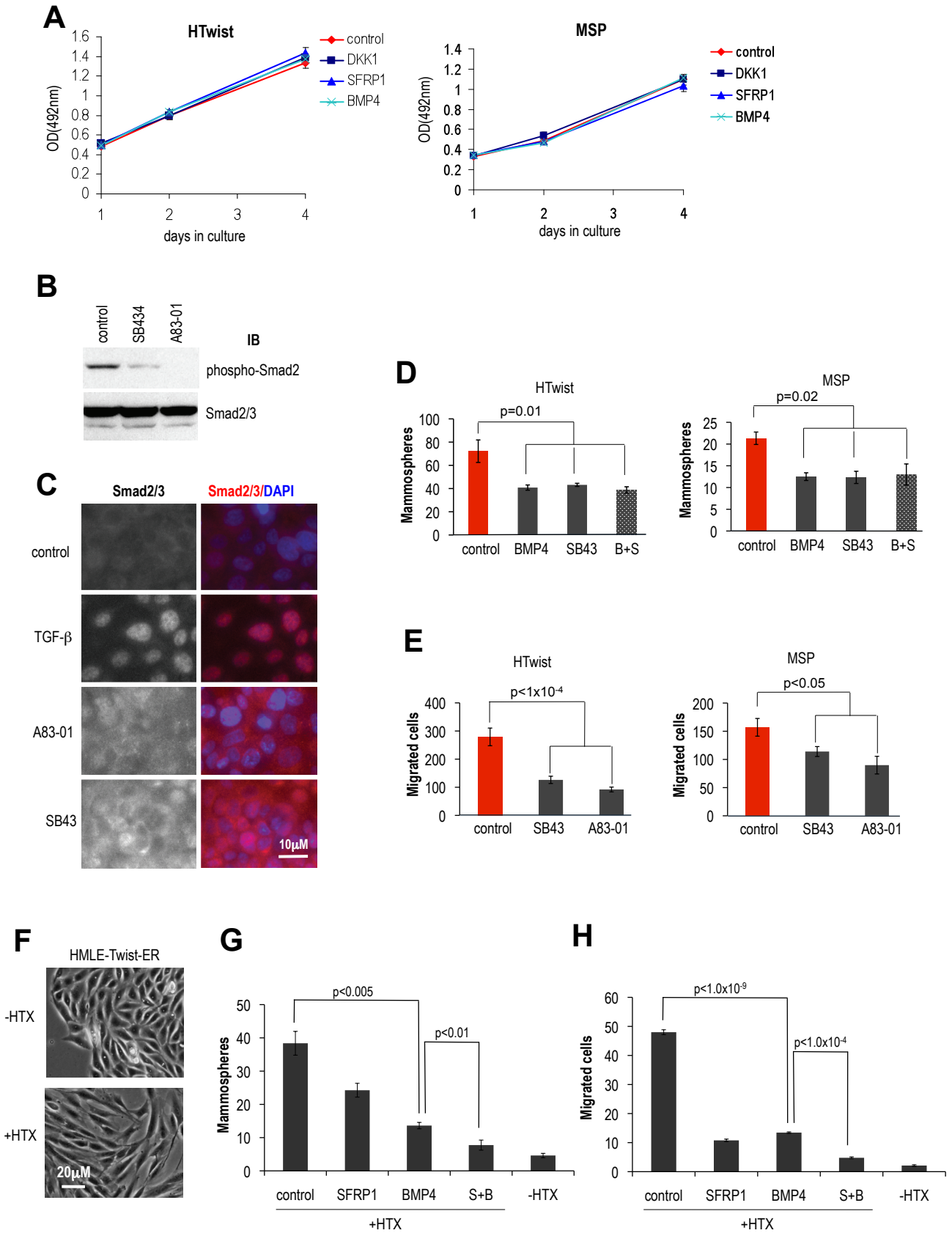


Figure S4

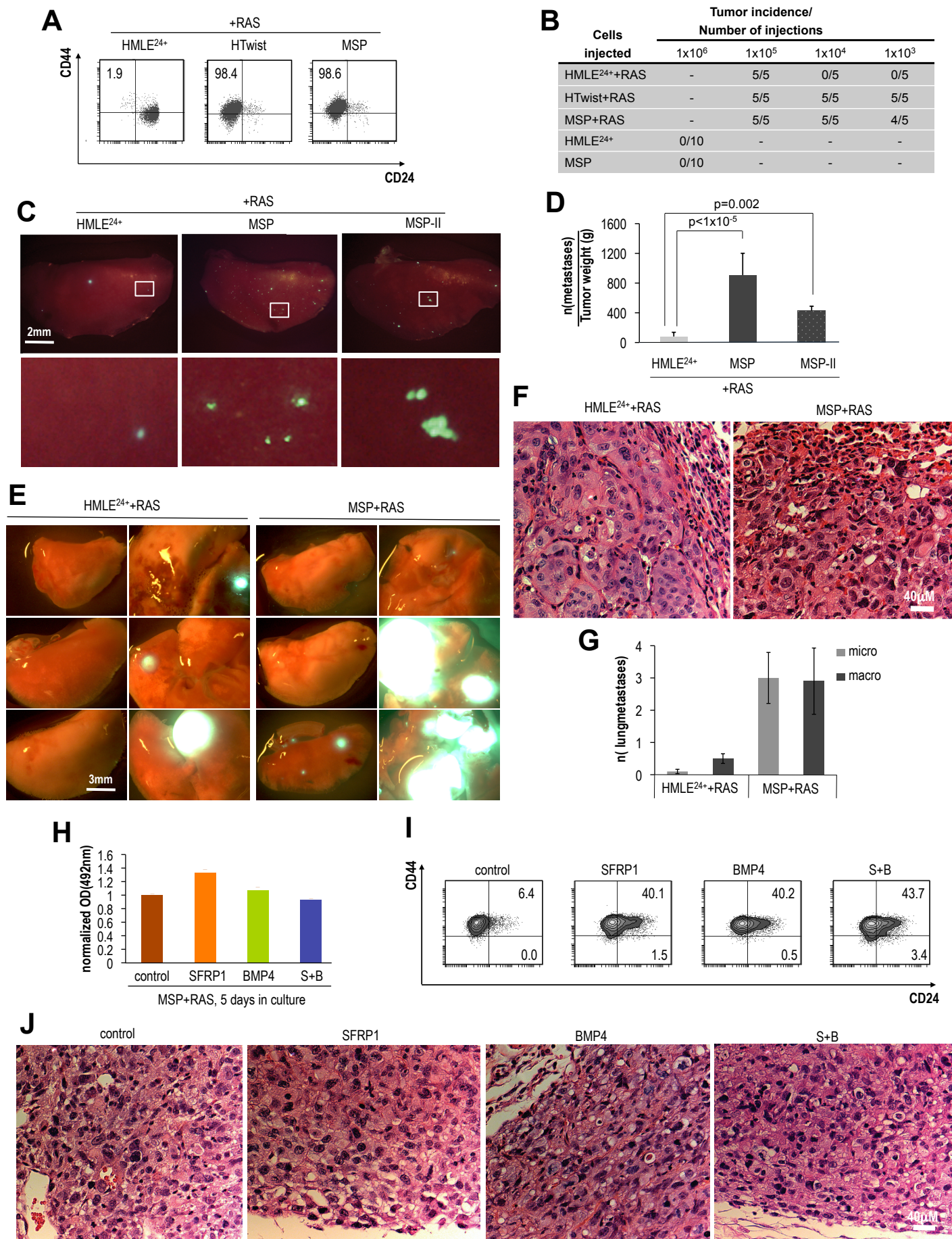


Figure S6

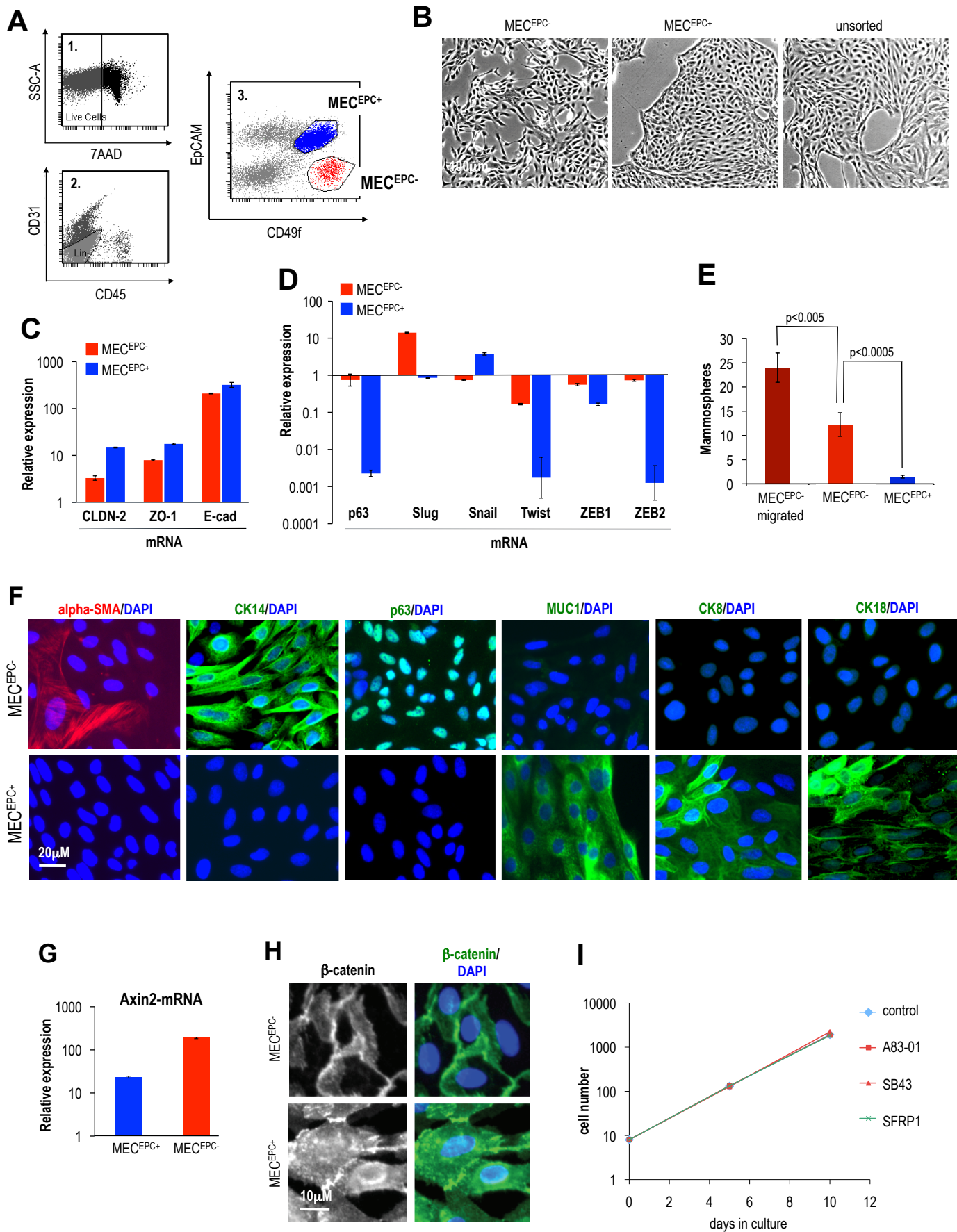


Figure S7

